Computational Materials Science 156 (2019) 246–251

Contents lists available at ScienceDirect

Computational Materials Science

journal homepage: www.elsevier.com/locate/commatsci

High-symmetry tin(II) iodides as promising light absorbers for solar cells: A theoretical prediction

Jessica Jein White, Junxian Liu, Yun Wang*

School of Environment and Science, Centre for Clean Environment and Energy, Griffith University, Gold Coast, QLD 4222, Australia

ARTICLE INFO

Keywords:
Lead-free light absorber
Tin(II) iodides
Band gap
Effective masses of charge carriers
Solar cells

ABSTRACT

While lead-based perovskite solar cells have advanced recently, the toxicity of lead brings its large-scale applications into question. Therefore, the discovery of lead-free light absorbers becomes of paramount importance. Tin has attracted intensive interest since it is another IVA element, which possesses the potential to replace lead. In this study, tin(II) iodides (SnI_2) with two different crystal structures were theoretically investigated using the first-principles density functional theory method. Our computational results reveal that the tetragonal SnI_2 with space group $P4_2/mnm$ has the band gap of 1.69 eV, which is close the optimal bandgap energy of 1.4 eV for the single junction solar cells. The further analysis of electronic properties of this tetragonal SnI_2 demonstrates that its valence band maximum includes dispersive *s* states of Sn, which is similar as that of Pb in the high-performance light absorbers. As such, the SnI_2 material may have the superior charge carrier transport rate as evidenced by the considerably small effective masses of photo-induced electrons and holes. Our findings, therefore, suggest that the novel high-symmetry tetragonal SnI_2 may be a promising candidate for photovoltaic applications.

1. Introduction

Organolead halide perovskites have emerged as a promising light absorber to realize low-cost and high-efficiency solar cells due to its specific structural, electronic and optical properties [1]. The efficiency of these Perovskite Solar Cells (PSCs) are rapidly increasing from an efficiency of 3.8% in 2009 to 22.7% recently [2]. Pb(II) cations in widely used organolead halide perovskites, e.g. $CH_3NH_3PbI_3$, has an occupied 6s state, which is very different from other metal cations. Theoretical studies have demonstrated that the unique electronic feature correlated with the Pb 6*s* pseudo-closed shell configuration is one of the major contributions to their superior photovoltaic properties.[3] Firstly, the filled Pb 6*s* state in the valance band maximum (VBM) hybridized with the I 5*p* states, which causes the conduction band minimum (CBM) is largely contributed by the Pb 6*p* states. Consequently, the intra-atomic Pb 6*s* to Pb 6*p* transition probability is high, which is beneficial to the optical absorption. Secondly, the hybridization of Pb 6*s* and I 5*p* states significantly increases the VBM level. Additionally, the I-I interactions in organolead perovskites are weak during the formation of defects due to their large ionic radius. Consequently, the antibonding p-p σ* state induced by I-I interactions is deeper than the VBM level, which can minimize the defect impacts on the performance of light absorption. Finally, the *s* states are more diffusive that the other states. As such, the existence of *s* states in the VBM can effectively lower the effective mass of holes, which will benefit the migration and separation of the photo-induced electrons and holes.

While organolead halides have the great advantage for solar cells, the concerns of the toxicity, bioavailability and water solubility of lead cast doubt on their commercialization [4]. To this end, numerous efforts have been devoted to replacing lead with other cations with the similar ns^2 electron configurations (lone pair *s* electrons), such as Sn^{2+}, Ge^{2+} and Bi^{3+} [5]. Amongst these, Sn^{2+} was demonstrated to be most promising [6]. Since the valence electron configuration of Sn^{2+} is $5s^2$, their VBM states are mainly Sn 5*s* hybridised with a component of halogen *p* states; and the main component of CBM of Sn(II)-based light absorbers can be unoccupied Sn *5p* states, which are similar to Pb(II) in the organolead perovskite halides. While the state-of-the-art solar-to-electricity conversion efficiency of Sn(II)-based solar cells is still much lower than that of Pb(II)-based ones [7], the possibility to use Sn to replace toxic Pb has already been experimentally confirmed. Therefore, the discovery of new Sn(II)-based light absorbers with desirable electronic and optical properties are imperative to accelerate the renovation of lead-free solar cells.

In this study, one of the simplest tin(II) halides, tin(II)) iodide (SnI_2), has been systematically investigated using the first-principles

* Corresponding author.
E-mail address: yun.wang@griffith.edu.au (Y. Wang).

https://doi.org/10.1016/j.commatsci.2018.09.058
Received 8 March 2018; Received in revised form 28 September 2018; Accepted 30 September 2018

density functional theory (DFT) method. From the Materials Project database, there are two possible SnI_2 crystal structures [8]. Our theoretical results reveal that the tetragonal SnI_2 with space group $P4_2/mnm$ possesses the desired electronic and optical properties, which has the potential to replace the toxic lead-based light absorbers for the photovoltaic application.

2. Computational details

All DFT computations were performed using the Vienna *ab initio* simulation package (VASP) based on the projector augmented wave (PAW) method [9,10]. Electron-ion interactions were described using standard PAW potentials, with valence configurations of $4s^24p^65s^24d^{10}5p^2$ for Sn (Sn_sv_GW) and $4s^24p^65s^24d^{10}5p^5$ for I (I_sv_GW). A plane-wave basis set was employed to expand the smooth part of wave functions with a cut-off kinetic energy of 520 eV. Two SnI_2 phases with the low symmetric monoclinic space group $C2/m$ and high symmetric tetragonal space group $P4_2/mnm$, which are termed as *mono*-SnI_2 and *tetra*-SnI_2, respectively, were investigated. The primary unit cell of *mono*-SnI_2 includes 6 Sn atoms and 12 I atoms. The primary unit cell of *tetra*-SnI_2 has 2 Sn atoms and 4 I atoms inside. Herein, three exchange-correlation (XC) functional, CA91 at the local density approximation (LDA) level [11], PBE at the generalized gradient approximation (GGA) level [12] and the DFT-D3 [13] with the consideration of the van der Waals force correction were selected to optimize the lattice constants and atomic structures due to their popularity and reliability. All the atoms were allowed to relax until the Hellmann-Feynman forces were smaller than 0.01 eV/Å. The convergence criterion for the electronic self-consistent loop was set to 0.00001 eV. We performed Brillouin-zone integrations using a gamma-centred (2 × 6 × 2) and (4 × 4 × 6) k-point grids for the *mono*-SnI_2 and *tetra*-SnI_2, respectively. Since the computations using the DFT method at the LDA and GGA levels generally have serious underestimated bandgap energies, the density of states (DOS) and band structures of SnI_2 were, therefore, computed using the HSE06 functional at the hybrid DFT level [14–16]. The screening parameter for exchange of the HSE06 functional was 0.2 $Å^{-1}$. An exchange functional of 20% exact HF exchange with 80% PBE exchange was employed in this study since calculations with such ratio accurately predicted the band gap of *mono*-SnI_2. Previous studies have demonstrated that the spin-orbital coupling (SOC) effect is insignificant since Sn is much lighter than Pb [17]. As such, the SOC effect was not considered in this study.

3. Results and discussion

3.1. Impact of exchange and correlation (XC) functionals

Our previous studies have demonstrated that the DFT XC functionals have considerable influence on the theoretical structural and electronic properties of the $CH_3NH_3PbI_3$ material [18]. In this regard, the impact of XC functionals on the structural properties of *mono*-SnI_2 was first evaluated. The *mono*-SnI_2 was selected since it has been experimentally synthesized [19]. Its experimental data can be used as the reference to evaluate the performance of XC functionals for SnI_2. The atomic structure of *mono*-SnI_2 is shown in Fig. 1.

The atomic structure of the *mono*-SnI_2 crystal is complex due to the low symmetry, which primary unit includes two types of Sn and three types of I atoms in terms to their chemical environments. Since there are several variables relevant to its total energy, both the lattice constants and atomic structures were optimised spontaneously. The optimised structural lattice constants and the corresponding experimental data are listed in Table 1. For all considered XC functionals, the *a* value is underestimated by 0.07–2.40%, which corresponds to an absolute error of 0.01–0.34 Å. The maximum error is with the CA91 functional, followed by DFT-D3 functional, with the PBE functional being the closest at 14.16 Å. The same trend was also observed for the values of the lattice constants *b* and *c*. On the other hand, the lattice angles are insensitive to the choice of XC functionals. Since the PBE results are most in agreement with the experimental lattice constants, the PBE functional was, therefore, chosen to optimize the atomic structure of the *tetra*-SnI_2 with space group $P4_2/mnm$, which has not been investigated so far. The thermodynamic stability of *tetra*-SnI_2 is evaluated based on its formation enthalpy values (ΔH_f), which is the difference between total enthalpies of products and reactants. Here, the formation enthalpy of SnI_2 can be through the reaction between Sn metal and I_2 molecule, e.g. $Sn + I_2 \rightarrow SnI_2$. The ΔH_f values of *tetra*-SnI_2 and *mono*-SnI_2 are −1.82 eV and −1.79 eV, respectively. The negative ΔH_f values suggest that both phases are thermodynamically stable. Moreover, the stability of *mono*-SnI_2 has been confirmed experimentally [19]. Thus, their almost identical ΔH_f values of these two phases confirms the high thermodynamic stability of *tetra*-SnI_2.

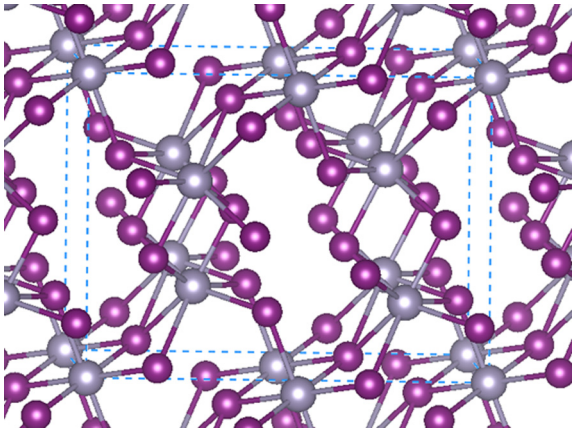

Fig. 1. Optimised atomic structure of *mono*-SnI_2 with the $C2/m$ space group. Key – purple: I and grey: Sn. (For interpretation of the references to color in this figure legend, the reader is referred to the web version of this article.)

Table 1
The performances of difference DFT XC functionals on the structural and electronic properties of mono-SnI_2 with the $C2/m$ space group.

	a (Å)	b (Å)	c (Å)	β (°)
CA91	13.83	4.29	10.23	92.8
PBE	14.16	4.39	10.84	92.4
DFT-D3	13.97	4.36	10.74	92.4
Exp.[a]	14.17	4.54	10.87	92.0

[a] The data from the Ref. [19].

3.2. Structural properties of tetra-SnI_2

In comparison with that of *mono*-SnI_2, the symmetry of *tetra*-SnI_2 is much higher including only one type of Sn and one type of I atoms (see Fig. 2). Thus, only two lattice constants *a* (which is equal to *b*) and *c* are variables to the total energies due to the high system. Based on the total energy potential over the lattice constants of *a* and *c* (see Fig. 2), the optimised *a* and *c* values are 7.59 Å and 4.73 Å, respectively. The optimization results demonstrated that the Sn—I bond in the *tetra*-SnI_2 phase is larger than that in the *mono*-SnI_2 crystal. In the *tetra*-SnI_2 phase, all the Sn—I bonds have the same length of 3.20 Å due to the high symmetry. As a comparison, the *mono*-SnI_2 crystal, has much various Sn—I bond lengths. The shortest and average Sn—I bond lengths are 3.05 Å and 3.16 Å, respectively, in the *mono*-SnI_2 crystal. The different structural properties indicate the electronic and optical properties of two phases may vary.